First analyses of planar magnetic structures associated with the Halloween 2003 events from the Earth to Voyager 1 at 93 AU

Devrie S. Intriligator,[1] Adam Rees,[2] and Timothy S. Horbury[2]

Received 2 August 2007; revised 18 December 2007; accepted 31 January 2008; published 9 May 2008.

[1] We perform the first analyses of planar magnetic structures beyond 5 AU. We also perform the first analyses of planar magnetic structures associated with the Halloween 2003 solar events. Our analyses show that planar magnetic structures (PMS) are associated with the interplanetary manifestation of the Halloween 2003 solar events over a wide range of heliocentric distances, heliolongitudes, and heliolatitudes. PMS are present at all five spacecraft (ACE, Ulysses, Cassini, Voyager 2, and Voyager 1); we investigate at distances ranging from the Earth to 93 AU. Our analyses indicate that generally the planes forming the PMS become better defined as they propagate farther out in the heliosphere. Also generally the cone angle of the PMS normal with respect to the radial direction decreases as the PMS propagate farther out in the heliosphere. This presence of PMS throughout the heliosphere is consistent with large-scale compressions associated with the interplanetary propagation of shocks and interaction regions and with possible consequences for cosmic ray and energetic particle modulation. In the case of Voyager 2, the PMS occur in the region after the main shock and are associated with enhanced interplanetary magnetic field magnitudes. This post shock region is associated with the modulation of galactic cosmic rays (>70 MeV/nuc). At Voyager 1 there is a ''textbook example'' of a PMS which also is associated with the modulation of galactic cosmic rays. It is tempting to associate these PMS with the ''propagating diffusive barriers'' of Wibberenz et al. (2002).

Citation: Intriligator, D. S., A. Rees, and T. S. Horbury (2008), First analyses of planar magnetic structures associated with the Halloween 2003 events from the Earth to Voyager 1 at 93 AU, *J. Geophys. Res.*, *113*, A05102, doi:10.1029/2007JA012699.

1. Introduction

[2] *Intriligator et al.* [2005] presented analyses of the propagation of the Halloween 2003 (19 October–20 November 2003) solar events throughout the heliosphere. Using the quick-look 3D HAFv2 model [*Fry et al.*, 2003; *Dryer et al.*, 2004]. *Intriligator et al.* [2005, 2006] found evidence of the asymmetric interplanetary propagation of the Halloween 2003 events. Figures 1a and 1b are from *Intriligator et al.* [2005] and show the longitudinal propagation of these events in the inner heliosphere (<10 AU) on 10 November 2003 and in the outer heliosphere (<100 AU) on 19 April 2004, respectively. The figures illustrate the deformation of the interplanetary magnetic field from the Parker spiral. Figure 1a shows that the events are propagating preferentially in the direction of the lower right quadrant. The heliocentric distance and longitudinal location of each of the three inner (<10 AU) heliospheric spacecraft are also shown. In Figure 1a the black dot in the lower right quadrant denotes the location of Earth and ACE. The locations of Ulysses and Cassini (i.e., ''Cas'') are shown in the upper right quadrant. Figure 1a indicates that on 10 November 2003, the shocks have passed Earth and that the innermost shock is approaching Ulysses. Cassini is between several major shocks and the weak flank of the innermost shock may eventually reach Cassini. The black dots in Figure 1b indicate the locations in the outer (<100 AU) heliosphere of Voyager 2 and Voyager 1 on 19 April 2004. The figure indicates that several shocks have propagated beyond Voyager 2 and another strong shock or merged interaction region is approaching Voyager 2. Figure 1b also indicates that on 19 April 2004, Voyager 1 is still in the ambient spiral interplanetary magnetic field and that a series of merged interaction regions or global merged interaction regions are approaching its longitude.

[3] The last two columns in Table 1 list the heliocentric distance and the latitude/longitude of each of the spacecraft. With the exceptions of Voyager 2 and Voyager 1, most of the spacecraft are relatively close to the ecliptic plane at this time. Voyager 2 is at 25 deg South and, in contrast, Voyager 1 is at 34 deg North. *Intriligator et al.* [2006] employed the full 3D MHD HHMS (Hybrid Heliospheric Modeling System) and presented additional evidence of the strong latitudinal and longitudinal asymmetries associated with the interplanetary propagation of the Halloween 2003 solar events.

[1] Carmel Research Center, Santa Monica, California, USA.
[2] Imperial College, London, England, UK.

0148-0227/08/2007JA012699

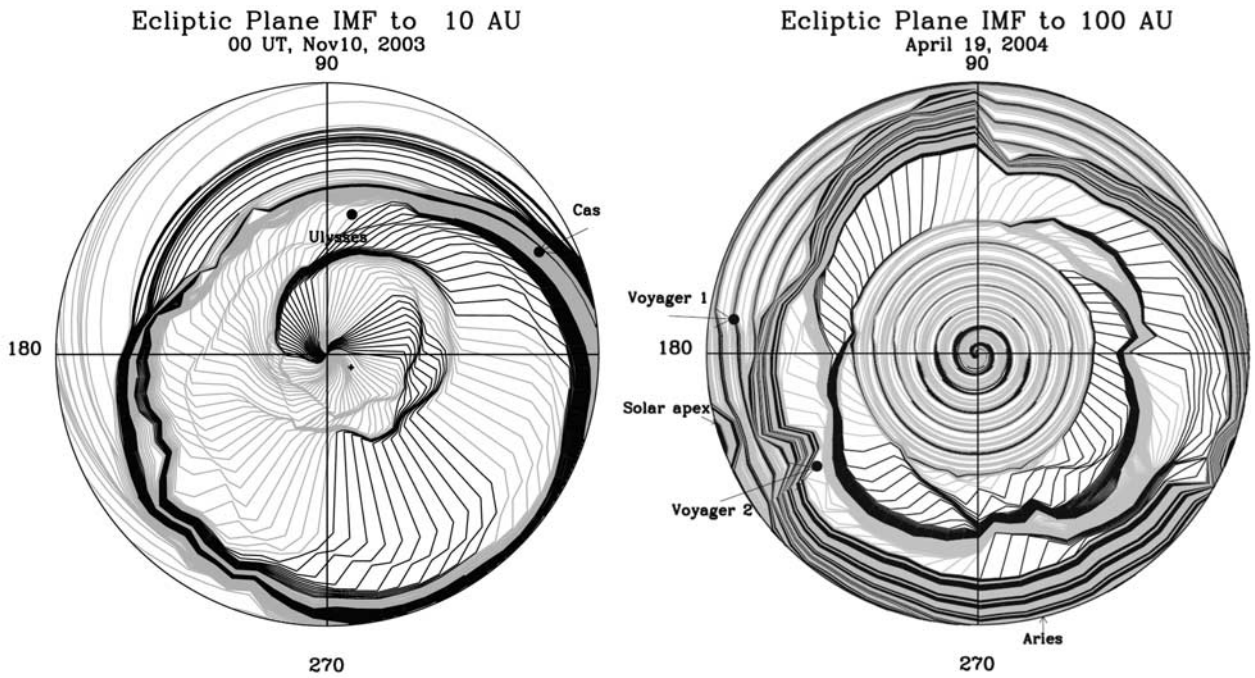

Figure 1. (a) Asymmetric interplanetary longitudinal propagation of the Halloween 2003 solar events to the inner heliosphere [*Intriligator et al.*, 2005] showing the ecliptic plane projection of interplanetary magnetic field (IMF) lines in heliographic inertial coordinates on 10 November 2003. The curved dark (light) lines show the IMF toward (away) sectors. These HAFv2 results show the distortions of the IMF lines from the spiral field configuration. The Sun is at the origin of the X axis. The radius extends to 10 AU. The small black dot at ~320 deg denotes the location of Earth and ACE. The positions of Ulysses and Cassini ("Cas") also are shown. The outermost shock has passed Cassini. This shock is much farther beyond Ulysses and another series of shocks is propagating toward Ulysses. See Table 1 for the specific spacecraft locations, including heliocentric distance, latitude, and longitude. (b) Same as Figure 1a, but showing for the Halloween 2003 solar events, using the same solar inputs as those used in Figure 1a, the HAFv2 model predictions for the interplanetary propagation in the IMF ecliptic plane out to 100 AU on 19 April 2004. The locations of Voyager 1 and 2 are shown. The figure indicates that a broad shock, probably associated with a merged interaction region from the Halloween 2003 solar events, passed the location of Voyager 2. The location of Voyager 1 is still immersed in the undisturbed spiral IMF.

[4] *Intriligator et al.* [2001] found evidence of PMS in corotating interaction regions (CIRs) in association with the stream interface and in association with the entire CIR. *Clack et al.* [2000] using Ulysses magnetic field data throughout two CIRs studied the three-dimensional structure and orientation of CIRs. *Intriligator et al.* [2001] showed that there was reduced cross-field transport for energetic particles near the stream interface in CIRs consistent with the energetic particle profiles and with the expectations of *Intriligator and Siscoe* [1994, 1995] and *Intriligator et al.* [1995]. *Intriligator et al.* [2005] showed that the Halloween 2003 events were both prolific producers of low energy particles and effective modulators of galactic cosmic rays (GCRs). In the present paper we continue to investigate the effects of the Halloween 2003 solar events on low energy particles and GCRs throughout the heliosphere.

[5] PMS were discovered by *Nakagawa et al.* [1989] and subsequently surveyed in the extensive Ulysses data set [*Jones and Balogh*, 2000, 2001]. It was found [*Jones and*

Table 1. Planar Magnetic Structures From ACE to Voyager 1[a]

S/C	Case (Normal)	Int/Min[b]	Max/Int[b]	R(AU)	Lat/Long[c]
ACE	A (−0.8, 0.6, 0.2)	6.67	1.53	1.0	4.5N/321.5
	B (−0.8, −0.2, −0.6)	5.46	1.21		
Ulysses	A (0.9, 0.2, 0.4)	6.34	3.17	5.2	5.8N/80
	B (0.9, 0.0, −0.4)	4.04	3.40		
Cassini	A (1.0, 0.0, −0.2)	13.73	1.51	8.7	3.5S/25.8
V2	A (0.7, −0.1, −0.7)	1.28	4.00	73.2	25.2S/215.3
	B (1.0, 0.0, 0.3)	1.83	4.79		
V1	A (−1.0, 0.0, −0.1)	20.68	2.96	93	34N/172.2

[a]Planar magnetic structures from ACE to Voyager 1. Summary of planar magnetic structures associated with the Halloween 2003 solar events as analyzed at ACE, Ulysses, Cassini, Voyager 2, and Voyager 1. Left column: s/c: spacecraft name; next (2nd) column: case: letter A or B for specific s/c PMS interval, as defined in figures. Normal: direction of PMS normal from minimum variance analysis. Int/min: ratio of intermediate to minimum eigenvalues from minimum variance analysis. Max/Int: ratio of maximum to intermediate eigenvalue ratios from minimum variance analysis. R(AU): s/c heliocentric distance in AU. Lat/Long: s/c latitude and longitude in degrees (HGI).

[b]Denotes eigenvalue ratios.

[c]Denotes degrees in HGI Heliographic Inertial coordinates.

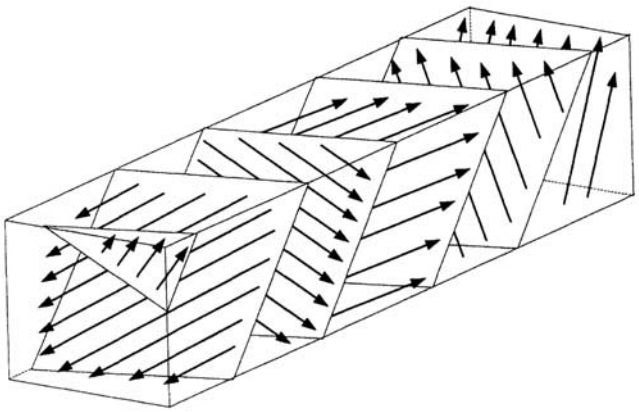

Figure 2. Planar magnetic structures (PMS) adapted from *Jones and Balogh* [2000]. B field vectors in neighboring regions, although oriented in various directions are all parallel to a fixed plane. Planar regions are separated by discontinuities, which also are parallel to the same plane.

Balogh, 2000, 2001] that PMS were present ~9–10% of the time when Ulysses was ±30 deg of the ecliptic at a distance of a few AU. They were less frequent at high latitudes [*Jones and Balogh*, 2000, 2001] and at 4-5 AU. It was speculated that they were less frequent at greater heliospheric distances. In contrast, we present the first evidence of the presence of PMS in the heliosphere at distances ranging from 1 to 93 AU.

2. PMS Analyses at ACE, Ulysses, Cassini, Voyager 2, and Voyager 1

2.1. Introduction

[6] As by *Intriligator et al.* [2001], we use minimum variance analysis [*Sonnerup and Cahill*, 1967] to determine the orientation of the PMS. Then the ratios of the intermediate to minimum eigenvalues were determined. The larger the value of this ratio, the greater the planarity of the PMS [*Jones et al.*, 1999]. Figure 2, adapted from *Jones and Balogh* [2000], is a conceptual drawing of planar magnetic structures (PMS). PMS can be formed in regions of compressions, such as CIRs and CMEs (coronal mass ejections), in which case the magnetic field vectors lie on a great circle in the location of the compression [*Intriligator et al.*, 2001].

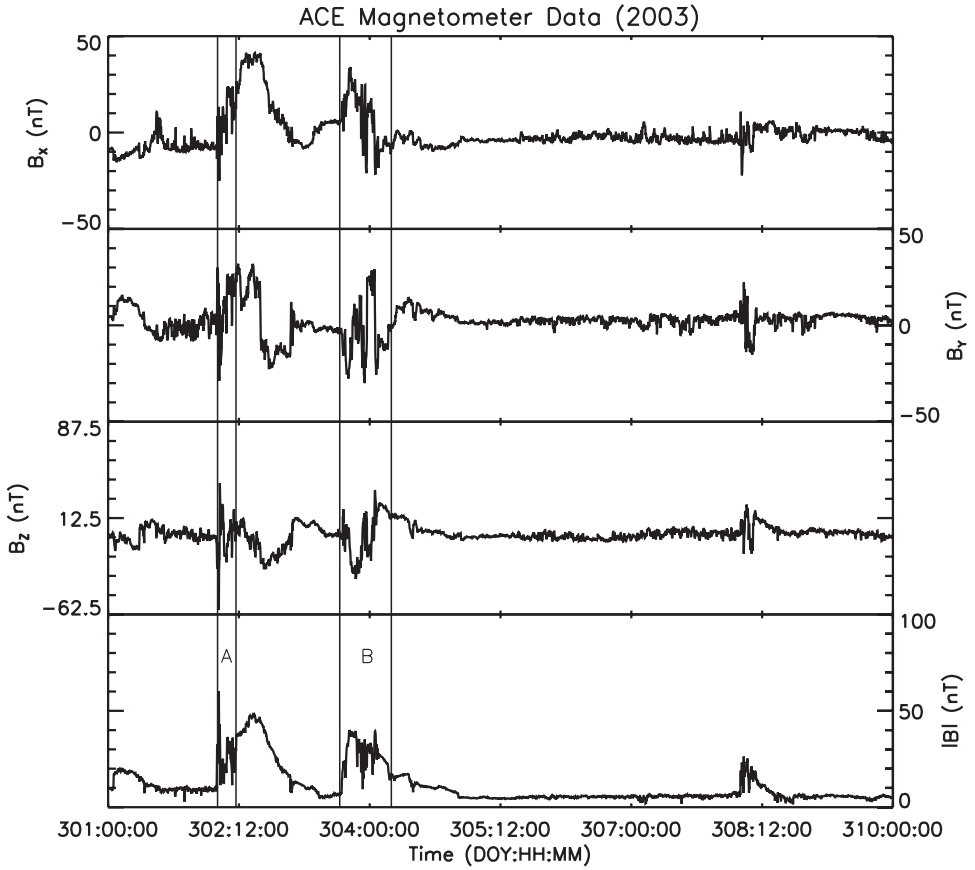

Figure 3. The arrival of the Halloween 2003 shocks at ACE on 28 (day 301), 29 (day 302), 30 (day 303) October and 3 (day 307) November 2003 are shown in the magnitude (in nT) of the interplanetary magnetic field (IMF) data (bottom panel). The three panels above the bottom panel show, respectively, the B_x, B_y, and B_z components of the IMF. The two intervals where PMS were found are indicated by A and B, with A referring to the interval from day 302.2549 to day 302.4660 and B referring to the interval from day 303.6552 to day 304.2471.

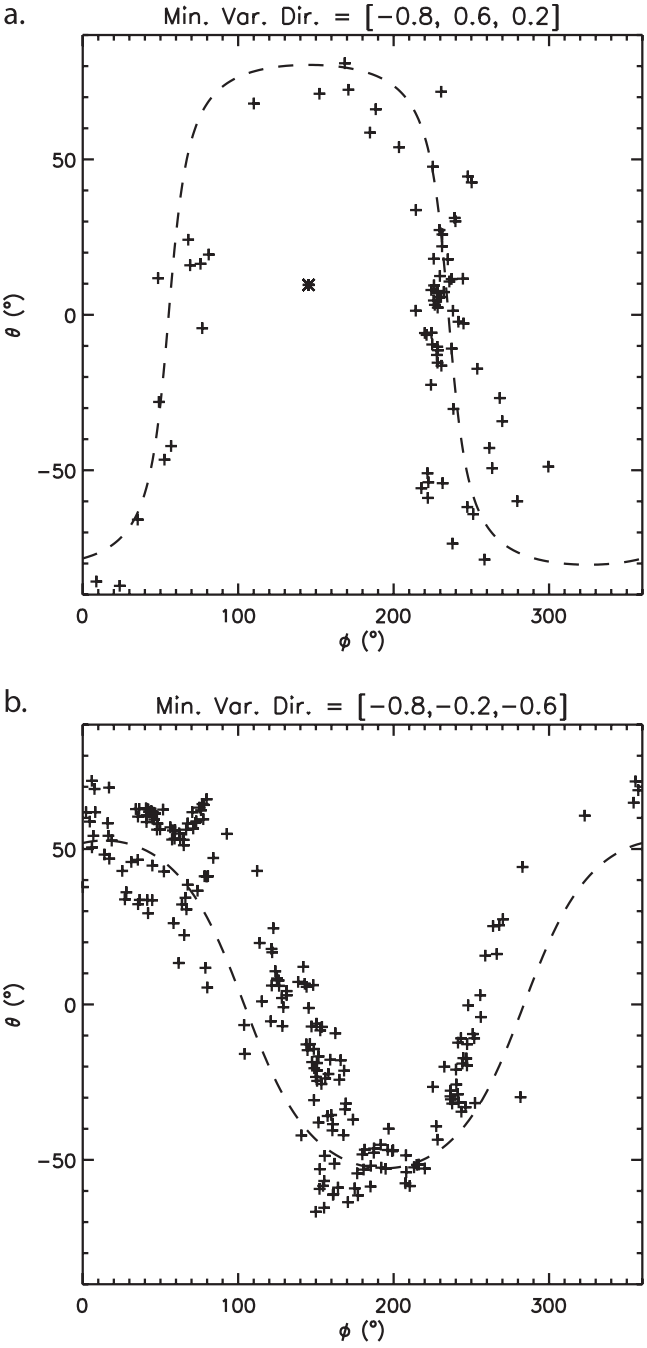

Figure 4. (a) PMS scatterplot of theta versus phi for the ACE PMS interval A shown in Figure 3. Table 1 lists some other relevant parameters associated with this and the other scatterplots shown below in this paper. (b) The same as Figure 4a, but for interval B shown in the ACE data in Figure 3.

Figure 2 shows that the magnetic field vectors in neighboring regions, although oriented in various directions are all parallel to a fixed plane. Planar regions are separated by discontinuities, which also are parallel to the same plane. The regions of search for PMS were selected by examining the obvious sheath regions in the data. Other regions of compression also were investigated.

2.2. PMS Analyses at ACE

[7] Figure 3 shows the time series interplanetary magnetic field (IMF) data of the Halloween events at ACE. These data are in the right-handed GSE (Geocentric Solar Ecliptic) coordinates where the +X axis points to the Sun, the Y axis is perpendicular to both the X and Z axes with the + direction opposite to the Earth's motion around the Sun, and the +Z axis points to the ecliptic north pole. The bottom panel in Figure 3 shows the IMF magnitude. The two time intervals (A and B) where PMS were identified are also labeled in this figure. As by *Intriligator et al.* [2001], we use scatterplots (see Figure 4) of IMF latitude theta angle versus IMF longitude phi angle to show the characteristic quasi-sinusoidal signatures of PMS illustrated by the dashed lines. In Figure 4 the scatterplots correspond to interval A (Figure 4a) and interval B (Figure 4b) in Figure 3. These two scatterplots employ 4-min resolution IMF data. In these two scatterplots it is clear that the data points lie along portions of the dashed lines which correspond to the orientations of the planar magnetic structures. The Figure 4a plot indicates that the PMS lies mainly along the 150 deg to 300 deg sector and that it is a planar structure. The Figure 4b plot shows the PMS generally follows the entire theta/phi plot from 0 deg to 360 deg. For the Figure 4a plot the minimum variance direction is [−0.8, 0.6, 0.2] and the ratio of the intermediate to minimum eigenvalues is 6.67. The maximum/intermediate eigenvalue ratio is 1.53. These values are summarized in Table 1 for all of the PMS examined in this paper. For the Figure 4b plot, the minimum variance direction is [−0.8, −0.2, −0.6] and the corresponding eigenvalue ratios are, respectively, 5.46 and 1.21. In both the cases in Figure 4, the large values of these ratios indicate that the field vectors tend to be close to a plane.

2.3. PMS Analyses at Ulysses

[8] Figure 5 is similar to Figure 3, but in the case of Figure 5 there is an extra panel at the bottom of the figure which displays the radial solar wind speed as measured by SWOOPS (i.e., the "solar wind observations over the poles of the Sun" experiment [*Bame et al.*, 1992] and the IMF components are in the RTN (Radial Tangential Normal) coordinate system. In this system the Sun is in the center and R points radially from the Sun to the spacecraft. T is perpendicular to R, and parallel to the solar equator, and points in the direction of orbital motion. N completes the system. Theta and phi are the latitude and azimuthal (longitudinal) angles in this system. As in the case of Figure 3, the two intervals investigated for PMS are labeled A and B. The scatterplots for these two intervals are shown in Figures 6a and 6b. As in the case of ACE, 4-min data are used in the Ulysses scatterplots. Both scatterplots in Figure 6 show the presence of PMS and the relevant quantities are summarized in Table 1.

2.4. PMS Analyses at Cassini

[9] Figure 7 is similar to Figure 5 except that Figure 7 does not include the solar wind speed at Cassini. On the basis of these IMF data at Cassini, it appears the interplanetary configuration is more complex at Cassini with the Halloween event mixed up with a CIR and the interval we want to investigate for the presence of PMS taken from the

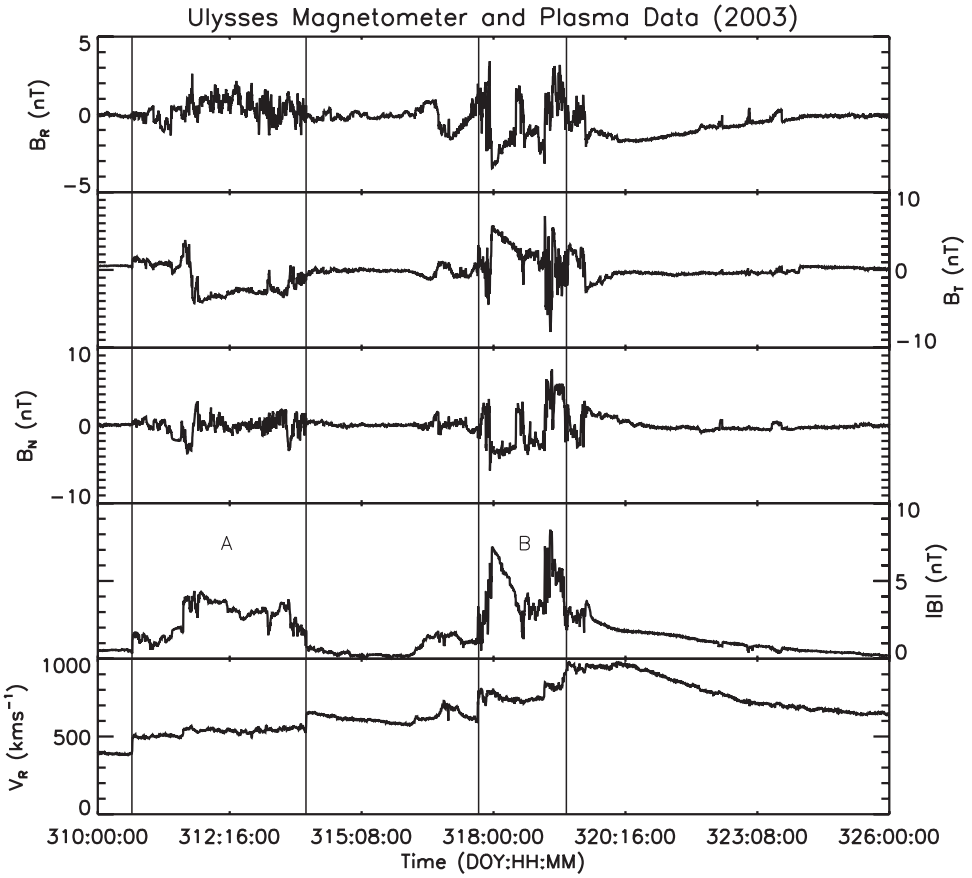

Figure 5. The same as Figure 3, but for Ulysses. The bottom panel shows Ulysses solar wind observations of the radial velocity V_R in km s^{-1}. The next panel is the same as the bottom panel in Figure 3 and shows the IMF magnitude at Ulysses during the Halloween events. The three top panels show the IMF components in the R, T, N coordinate system. The two intervals of PMS investigated in the Ulysses IMF data are indicated by A and B, with A referring to from day 310.6910 to 314.2094 and B referring to from day 317.6969 to 319.4707.

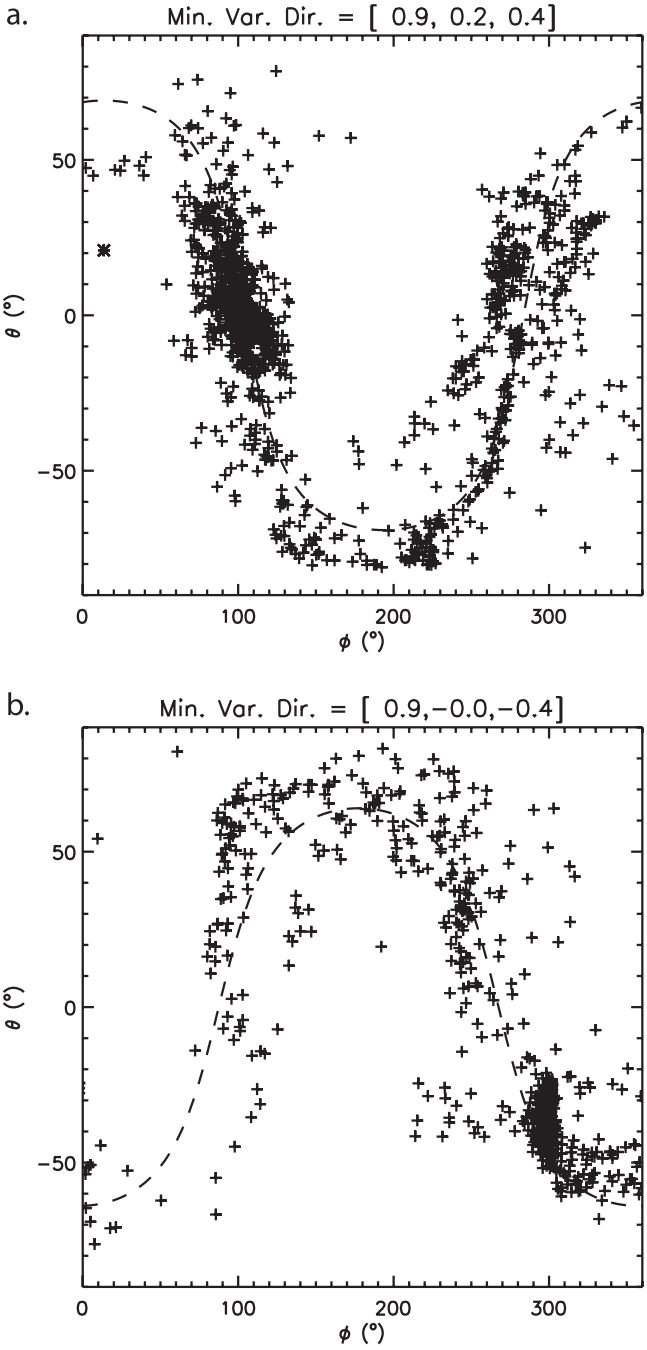

Figure 6. (a) PMS scatterplot of theta versus phi for the Ulysses PMS interval A shown in Figure 5. (b) The same as Figure 6a, but for interval B shown in the Ulysses data in Figure 5.

sheath region ahead of a magnetic cloud. Figure 8 uses 1-min resolution IMF data and clearly shows the presence of the PMS as summarized in Table 1.

2.5. PMS Analyses at Voyager 2

[10] Figure 9 is similar to Figure 7 and shows the two time intervals (A and B) we investigated where we found evidence for the presence of PMS in the IMF data at Voyager 2. In addition we investigated two other time intervals where we did not find evidence for PMS at Voyager 2: day 108.9981 to 118.4951 and day 117.8620 to 124.1933. The time resolution for the Voyager 2 IMF data is 1-h. The theta/phi plots for the two time intervals that did not show the presence of PMS are shown in Figures 10a and 10b. The minimum variance directions were [−0.7, 0.5, 0.4] and [0.1, −0.3, −1.0], respectively. It is evident in Figures 10a and 10b that the data points do not fall along most of the characteristic quasi-sinusoidal dashed line. In contrast, Figures 11a and 11b show the presence of PMS in intervals A and B with more of the data points falling closer to longer segments of the dashed curve. The quantities associated with intervals A and B at Voyager 2 where the PMS were present are listed in Table 1. The low (<2) Int/Min ratio for the two PMS intervals at Voyager 2 would usually indicate that the normal to the plane of the PMS is not well defined.

2.6. PMS Analyses at Voyager 1

[11] Figure 12 is similar to Figure 9 and shows the 1-h resolution IMF data at Voyager 1 and the interval A we investigated and found strong evidence for the presence of a planar magnetic structure. The PMS scatterplot is shown in Figure 13. The beautiful PMS shown in Figure 13 is quite remarkable in that it adheres to the PMS dashed line so closely. This is also indicated in Table 1 by the 20.68 Int/Min eigenvalue ratio where the high value for the ratio indicates the normal is well defined and the points closely lie in the PMS plane.

3. Discussion

[12] We have performed the first analyses of planar magnetic structures throughout the heliosphere associated with the Halloween 2003 solar events. We also have performed the first analyses of planar magnetic structures beyond the orbit of Jupiter (>5 AU). Table 1 summarizes the information on the planar magnetic structures associated with the Halloween 2003 solar events from ACE to Voyager 1. The heliocentric distance, latitude, and longitude of each spacecraft is also shown in Table 1. Generally, Table 1 shows that as the PMS move to greater heliocentric distances the orientation of their planes become more normal to the radial direction. Our analyses also indicate that, generally, the planes forming the PMS become better defined as they propagate farther out in the heliosphere (i.e., the intermediate/minimum eigenvalue ratio increases). Figure 14 illustrates the changing cone angle of the PMS normal as a function of heliocentric distance. The number of PMS events being plotted in this figure is limited to those studied in this analysis, and the apparent strength of the relationship between cone angle and distance is therefore limited. In the case of Voyager 1, the high intermediate/minimum eigenvalue ratio (see Table 1) and the cone angle of the normal of the PMS (see Figure 14) illustrate the presence of an extremely planar highly compressed PMS propagating radially outward at 93 AU and at 34 deg North.

[13] As shown in Table 1 and Figure 14, the exception to this trend of increased planarity and decreasing cone angle of the PMS normal with increasing heliocentric distance is Voyager 2 where the intermediate/minimum eigenvalue ratios are quite low (e.g., 1.28 and 1.83, for intervals A and B, respectively) and the cone angles of the PMS

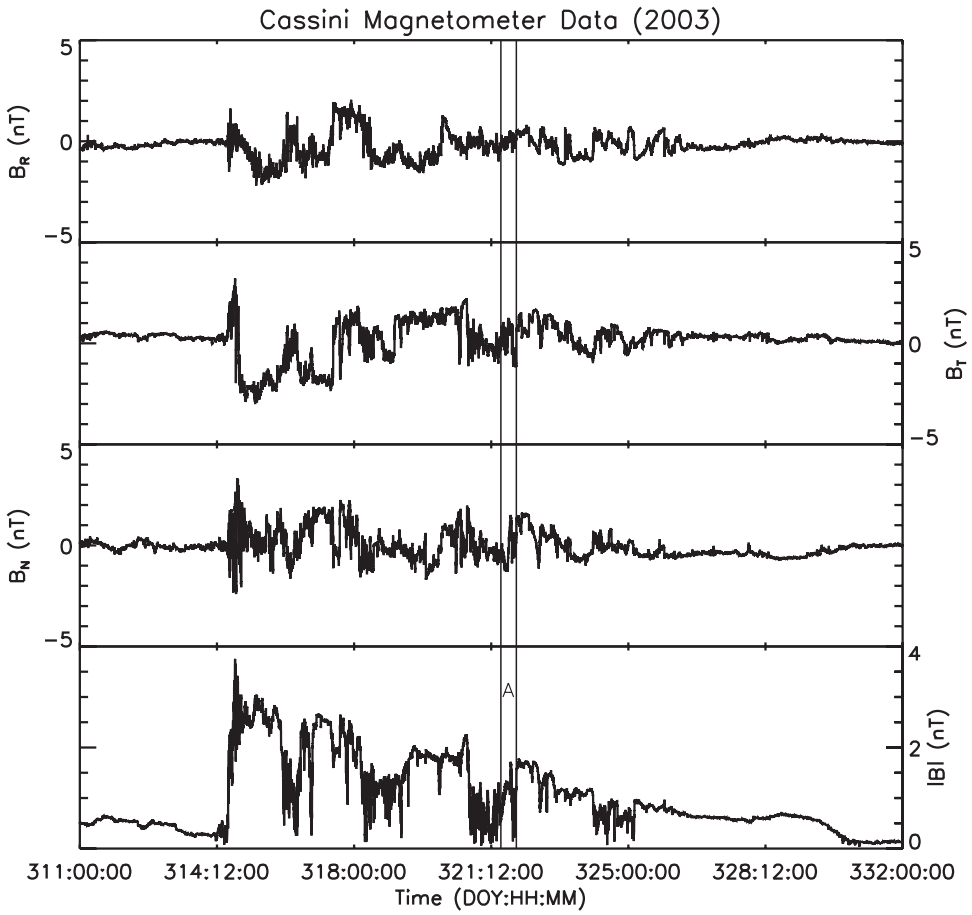

Figure 7. The same as Figure 5, but at the Cassini spacecraft. There are no in situ solar wind plasma data available from Cassini. The interval where PMS were found is indicated by A and refers to the interval from day 321.7455 to day 322.1409.

normals with respect to the radial direction are quite high. The Voyager 2 points in Figure 14 are clearly outliers and break the trend of decreasing cone angle of the PMS normals with respect to the radial direction with increasing heliocentric distance. For completeness we note, that *Jones et al.* [1999] reported that based on the available Ulysses data at <3 AU, the orientation of the Ulysses PMS planes were associated primarily with being perpendicular to the radial direction rather than parallel to the Parker spiral. While we were able to find PMS at Voyager 2, they were not associated with the primary large shock. It is possible that the quality of the Voyager 2 IMF data is not as high as that of the Voyager 1 IMF data and the other spacecraft IMF data due to larger uncertainties associated with correcting for magnetometer instrument offsets in the presence of the relatively weak ambient IMF in the outer heliosphere. It is also possible that the differences between the Voyager 2 PMS results and those of the other spacecraft are attributable to a latitude asymmetry in the South. For example, it is possible that the probable asymmetric blunt shape of the heliosphere where the termination shock resides at smaller heliocentric distances in the South may affect these parameters. In this case, however, one might speculate that this could lead to greater compression in the South at a given heliocentric distance and, thus, one would expect smaller cone angles of the PMS normals and more planarity (due to

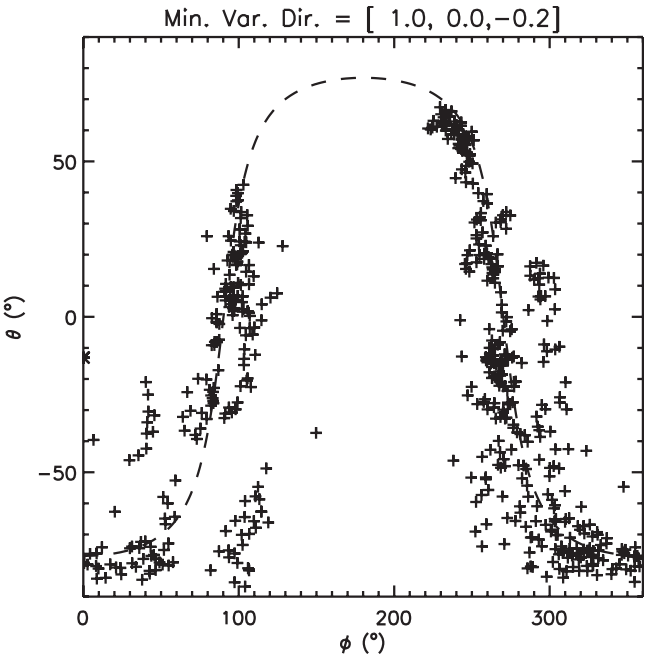

Figure 8. PMS scatterplot of theta versus phi for the Cassini PMS interval A shown in Figure 7.

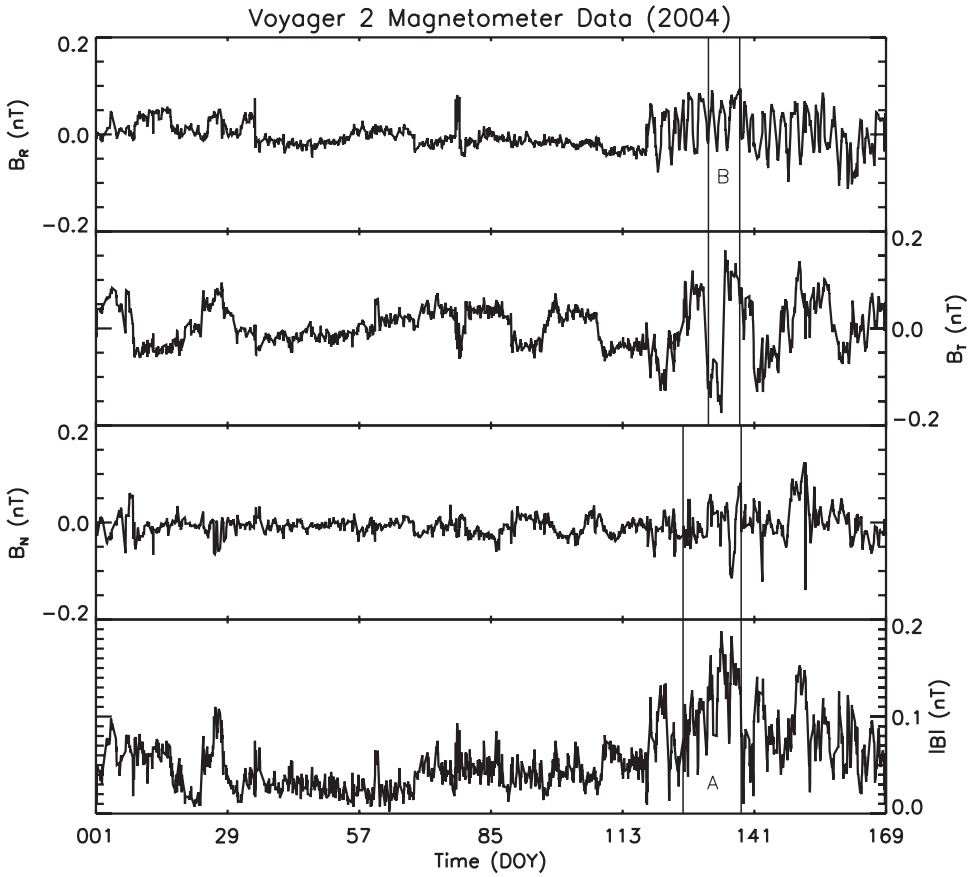

Figure 9. The same as Figure 7, but at the Voyager 2 spacecraft. The two intervals where PMS were not found were from day 108.9981 to 118.4951 and from day 117.8620 to 124.1933. The two intervals where PMS were found are indicated by A and B, with A referring to the interval from day 125.7585 to day 138.1655, and B referring to from day 131.1667 to day 137.8474.

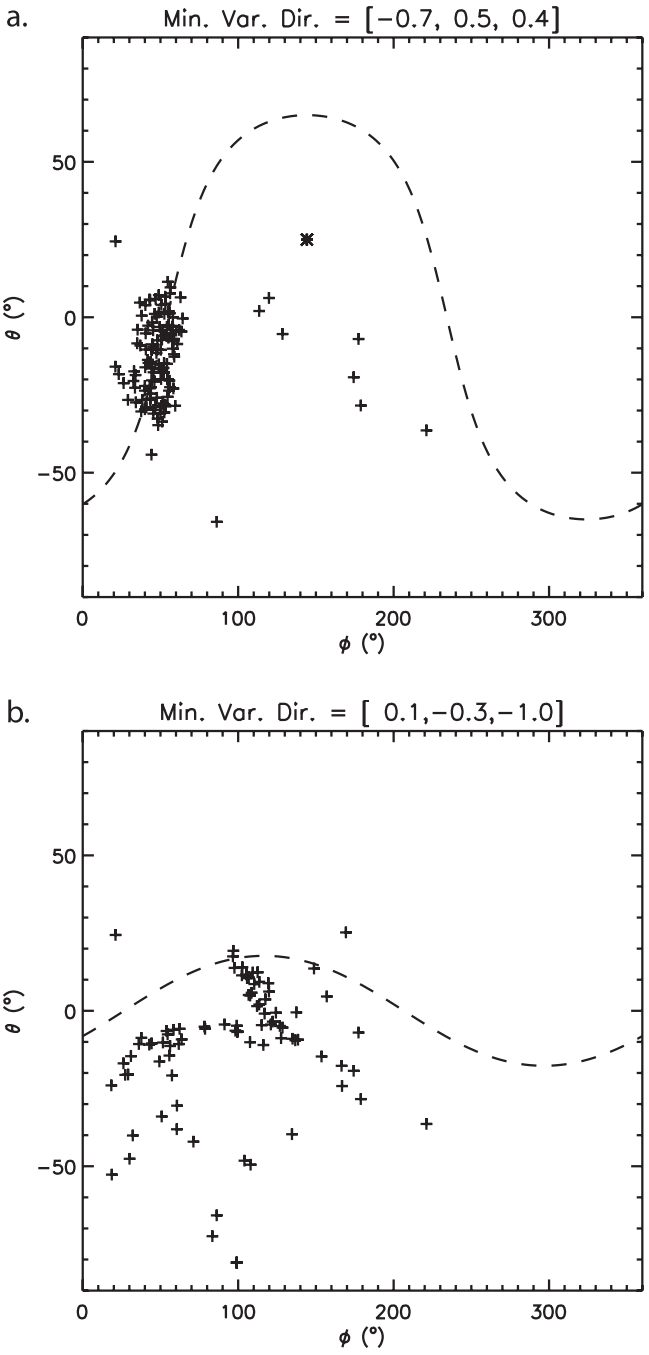

Figure 10. (a) Scatterplot of theta versus phi for the first Voyager 2 non-PMS interval: from day 108.9981 to day 118.4951. (b) The same as Figure 10a, but for the second Voyager 2 non-PMS interval: from day 117.8620 to day 124.1933.

more compression) in the South, in contrast to the larger cone angles of the PMS normals and less planarity that is observed at Voyager 2. We plan to investigate the implications of the Voyager 2 outliers in this PMS analysis in the future.

[14] In Figure 15 the downward pointing vertical arrow above the Voyager 2 speed data indicates the location on 28 April 2004 of the primary large shock associated with the arrival of the Halloween 2003 events at Voyager 2. No PMS were found when we tested for their presence during April 17.9–27.5, 2004 (the interval in Figure 10a) and April 26.9–May 3.2 (the interval in Figure 10b). In contrast, the Voyager 2 PMS were found following the primary large shock and were associated with the largest IMF magnitude features, as shown in the uppermost graph in Figure 15 and also in Figure 9. The two intervals during which PMS were present were: May 4.8–17.2, 2004 (interval A - see Figures 9 and 11a) and May 10.2–16.8, 2004 (interval B -

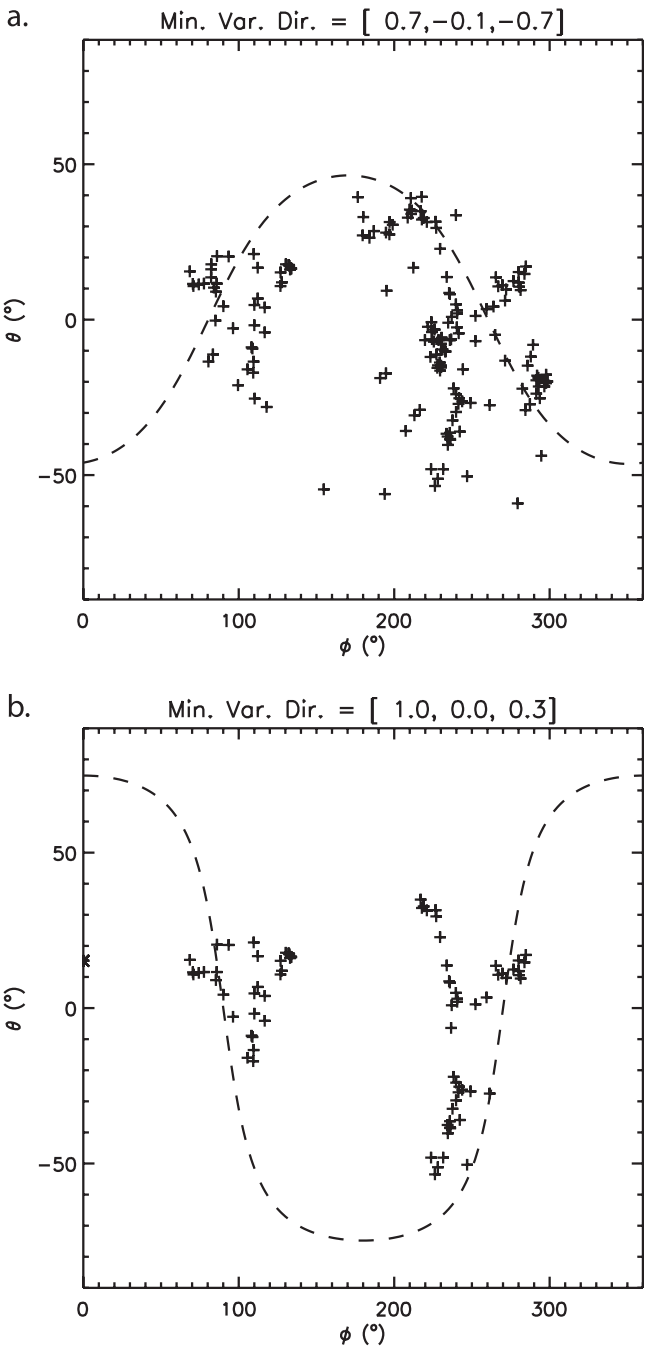

Figure 11. (a) Scatterplot of theta versus phi for interval A, the first Voyager 2 PMS interval shown in Figure 9. (b) The same as Figure 11a, but for interval B, the second Voyager 2 PMS interval shown in Figure 9.

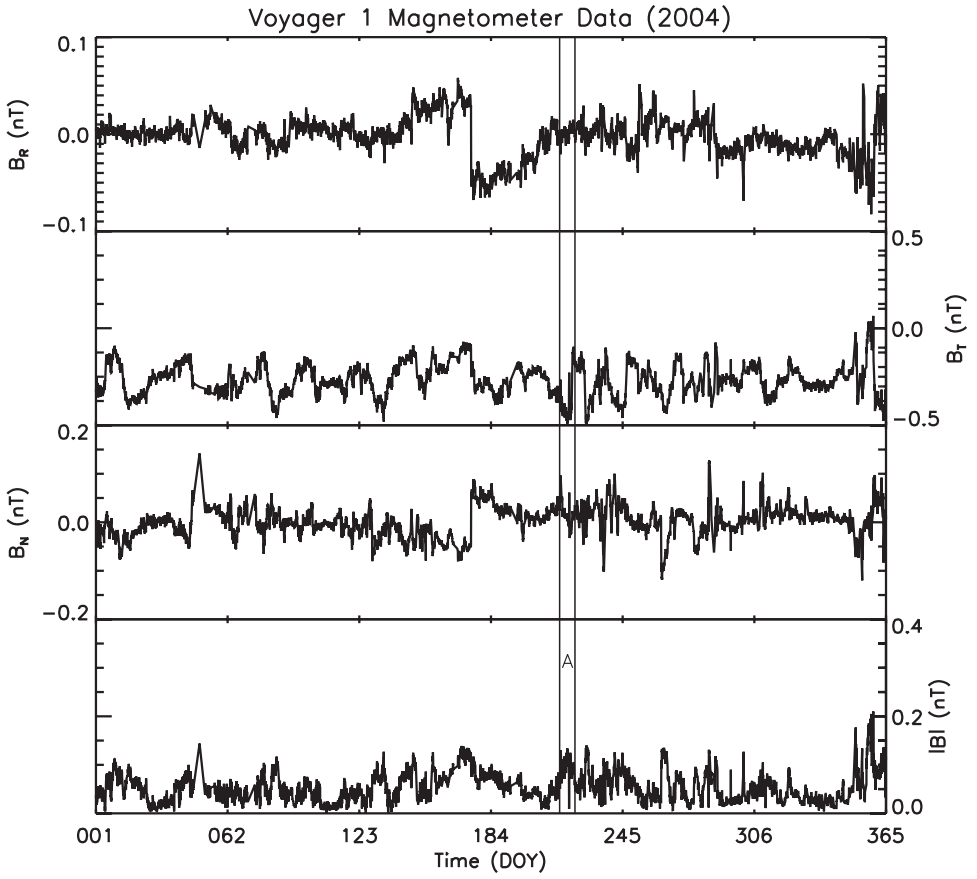

Figure 12. The same as Figure 9, but at the Voyager 1 spacecraft. The interval where PMS were found is indicated by A referring to the time period from day 213.6982 to day 220.7489.

see Figures 9 and 11b). The increased magnetic field magnitude and the presence of PMS also appear to be associated at Voyager 2 with the modulation of GCRs, as indicated in Figure 15 by the decrease in intensity of >70 MeV/nuc ions [*Intriligator et al.*, 2005, 2006]. The inclined upward pointing arrow below the Voyager 2 GCR (>70 Mev/nuc) data in Figure 15 indicates this interval of GCR modulation. This interval also corresponds to the highest solar wind speeds, as shown in the bottom panel of Figure 15. The Voyager 2 arrival of the primary large shock associated with the Halloween 2003 events was preceded by the increased intensities of the 2–3 MeV hydrogen ions. These energetic particles were accelerated at the shock. Following the peak IMF magnitudes in early May and during the intervals when the PMS were present, the intensities of the 2–3 MeV hydrogen ions began to steadily decrease in intensity. The increased IMF magnitude, the presence of planar magnetic structures, and the decreases in the intensities of GCRs and 2–3 MeV H are all consistent with the arrival of a region of strong compression associated with the Halloween 2003 events.

[15] *Intriligator et al.* [2001] showed that there was a reduction in cross-field transport for energetic particles associated with the strong compression near the stream interface of CIRs in the vicinity of PMS. Examination of the Voyager 1 IMF, GCRs, and energetic particle data in Figure 15 indicates that compression and the presence of the PMS may also play an important role in the GCR and

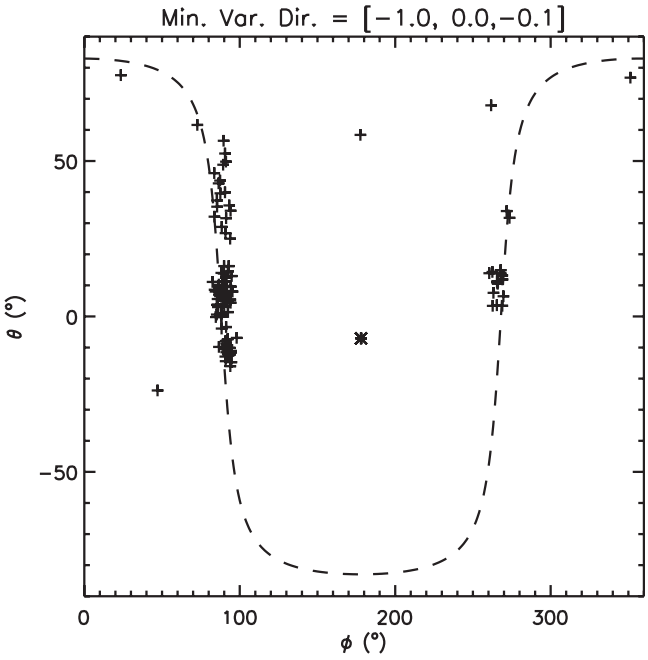

Figure 13. PMS scatterplot of theta versus phi for Voyager 1 PMS interval A shown in Figure 12. This is a remarkably beautiful PMS, as substantiated by the associated parameters listed in Table 1.

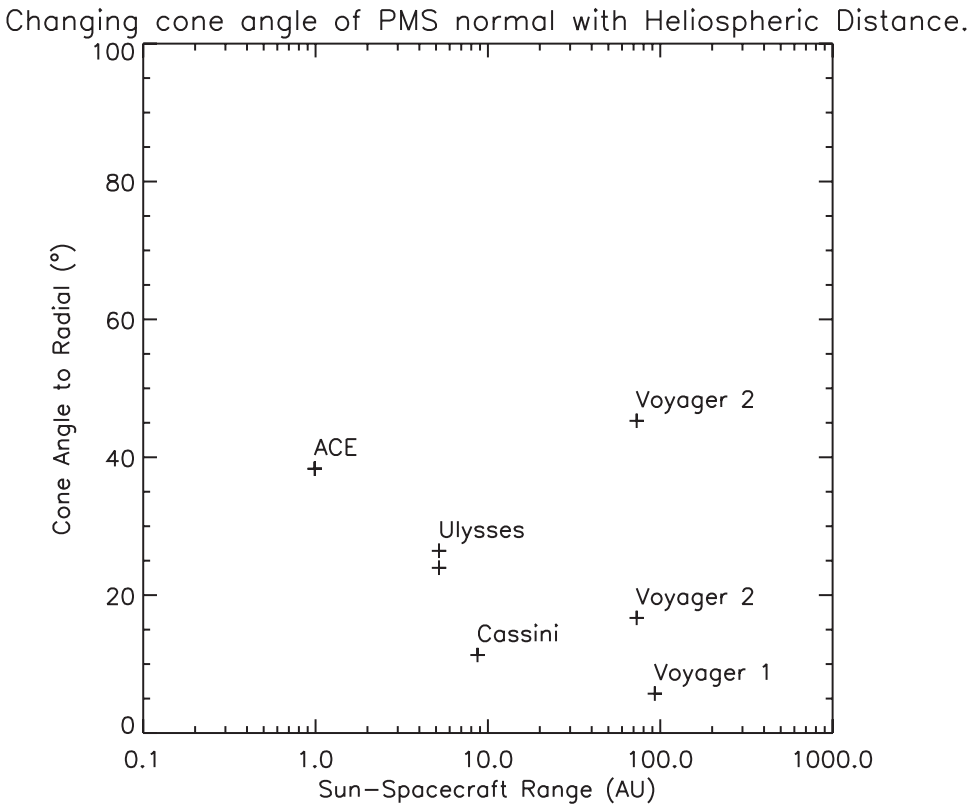

Figure 14. Changing cone angle of PMS normal as a function of heliocentric distance. Note the general trend of the decreasing cone angle to the radial with increasing heliocentric distance. The Voyager 2 PMS cone angles are outliers and may be indicative of a problem in the quality of the Voyager 2 IMF data or they could reflect a latitude asymmetry associated with the compression in the outer heliosphere and the propagation of PMS.

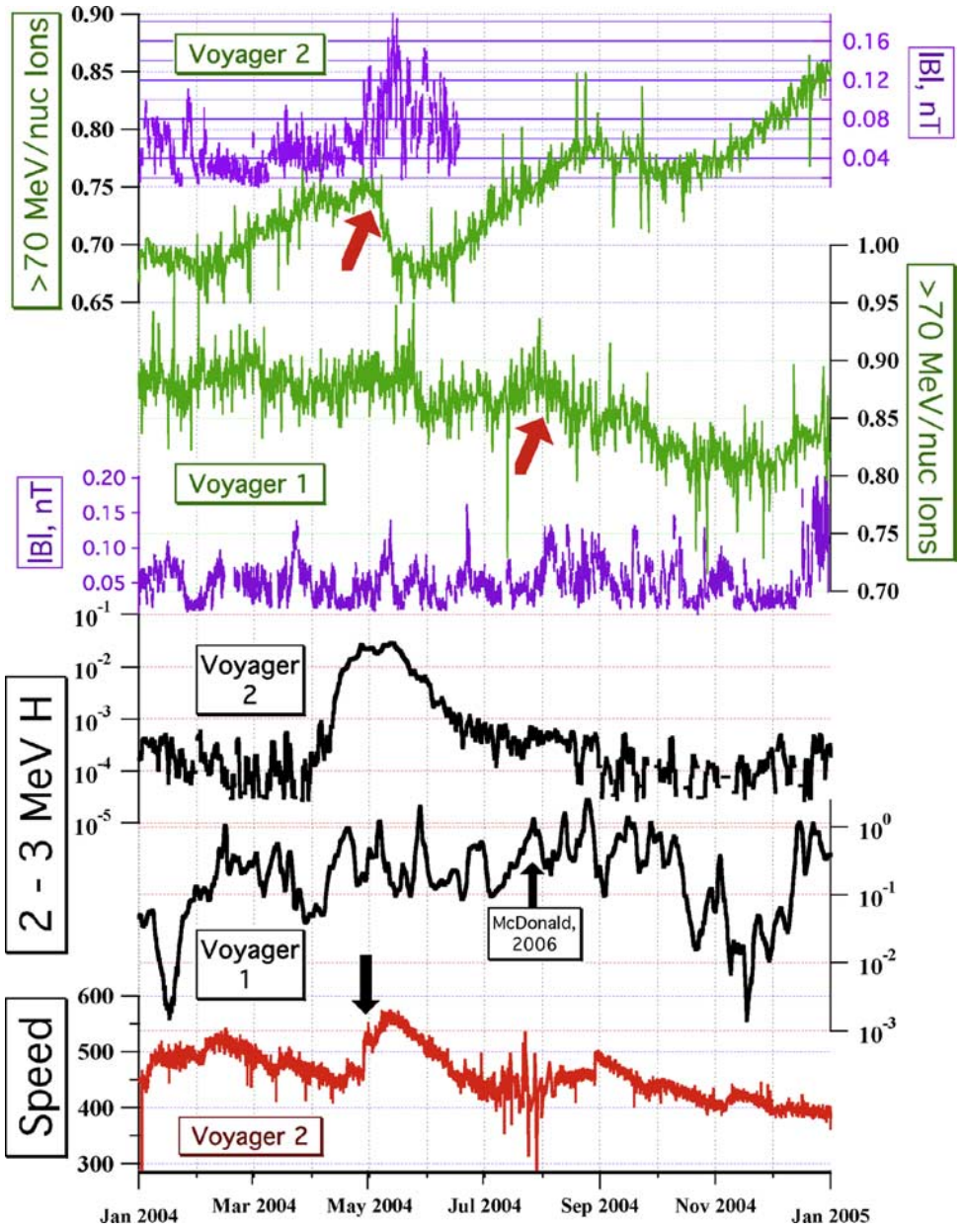

Figure 15. Voyager 1 and Voyager 2 data adapted from *Intriligator et al.* [2005, 2006]. The downward pointing vertical arrow above the Voyager 2 plasma speed data indicates the 28 April 2004 arrival of the primary large shock associated with the Halloween 2003 events. The inclined upward pointing arrow below the Voyager 2 GCR (>70 Mev/nuc) data indicates the interval of GCR modulation which also is associated with the presence of PMS at Voyager 2. This interval is also associated with the highest IMF magnitudes, as shown in the uppermost curve. This interval also corresponds to the highest solar wind speeds, as shown in the bottom panel of Figure 15. The inclined upward pointing arrow below the Voyager 1 GCR (>70 Mev/nuc) data indicates the interval of GCR modulation at Voyager 1 associated with the Halloween 2003 events. The upward pointing vertical arrow below the 2–3 MeV H Voyager 1 data indicates the arrival of the Halloween 2003 events at Voyager 1 as reported by *Intriligator et al.* [2005] and confirmed by *McDonald* [2006] and *McDonald et al.* [2006]. The sharp drop off of the particle intensity of this peak appears to be associated with the rapid increase of IMF magnitude at Voyager 1 (shown in the corresponding B (nT) curve displayed below the Voyager 1 GCR data) and with the arrival of the PMS.

energetic particle behavior at Voyager 1 in association with the Halloween 2003 events. The inclined upward pointing arrow below the Voyager 1 GCR (>70 Mev/nuc) data in Figure 15 indicates the modulation of the GCRs at Voyager 1 [*Intriligator et al.*, 2005]. The onset of the Voyager 1 GCR modulation appears to be associated with the increased IMF intensity, as shown in the curve immediately below these GCR data. The presence of the PMS at Voyager 1 during the interval July 31.7–August 7.7, 2004 (interval A - see Figures 12 and 13) is consistent with the compression of the field due to the CMEs associated with the Halloween 2003 solar events. The reader will recall the ''textbook'' Voyager 1 PMS shown in Figure 13, its extremely small cone angle shown in Figure 14, and the striking planarity of the Voyager 1 PMS also indicated by the high eigenvalue ratio in Table 1.

[16] Comparisons with the 2–3 MeV hydrogen ion intensities at Voyager 1 lead to interesting associations. The vertical upward pointing arrow (labeled ''McDonald, 2006'') below the 2–3 MeV H plot for Voyager 1 in Figure 15 indicates the arrival near the end of July 2004 of the Halloween 2003 events at Voyager 1 as reported by *McDonald* [2006], *McDonald et al.* [2006] and *Intriligator et al.* [2005]. Comparisons between these particle intensities and the Voyager 1 IMF magnitude data imply that the rather sharp decrease in particle intensity at the very end of July is associated with the rapid rise in IMF magnitude and with the arrival of the PMS. The interval of PMS presence appears to correspond to the interval of decreased 2–3 MeV H intensities at the beginning of August 2004. In addition, there appears to be an anti-correlation between the IMF magnitude and the 2–3 MeV H intensities that then persists for approximately the next month through the beginning of September 2004. As in the case of Voyager 2 discussed above, these Voyager 1 features in the IMF, PMS, GCRs, and 2–3 MeV H also are consistent with the conclusions of *Intriligator et al.* [2001] and reduced particle cross-transport due to compressions associated with the propagation of interplanetary events. It is tempting to associate the presence of PMS and the concurrent galactic cosmic ray modulation with the ''propagating diffusive barriers'' of *Wibberenz et al.* [2002]. In the future we plan to further investigate the intensity variations in GCRs and lower energy energetic particles and their associations with other interplanetary phenomena by performing some additional analyses including some similar to those we carried out in association with the stream interfaces in CIRs.

[17] **Acknowledgments.** The authors thank the ACE, Ulysses, Cassini, and Voyager magnetometer experimenters for the use of their data, D. McComas for the Ulysses plasma data, E. C. Stone for the Voyager CRS data, and the NSSDC for the COHO data sets. The work at CRC was supported by Carmel Research Center. Heliophysics research at Imperial College London is supported by the Science and Technology Facilities Council (UK). The authors appreciate the reviewers' comments.

[18] Zuyin Pu thanks the reviewers for their assistance in evaluating this paper.

References

Bame, S. J., D. J. McComas, B. L. Barraclough, J. L. Phillips, K. J. Sofaly, J. C. Chavez, B. E. Goldstein, and R. K. Sakurai (1992), The Ulysses solar wind plasma experiment, *Astron. Astrophys. Suppl.*, *92*(2), 237.

Clack, D., R. J. Forsyth, and M. W. Dunlop (2000), Ulysses observations of the magnetic structure within CIRs, *Geophys. Res. Lett.*, *27*(5), 625–628.

Dryer, M., Z. Smith, C. D. Fry, W. Sun, C. S. Deehr, and S.-I. Akasofu (2004), Real-time shock arrival predictions during the ''Halloween 2003'' epoch, *Space Weather*, *2*, S09001, doi:10.1029/2004SW000087.

Fry, C. D., M. Dryer, Z. Smith, W. Sun, C. Deehr, and S. Akasofu (2003), Forecasting solar wind structures and shock arrival times using an ensemble of models, *J. Geophys. Res.*, *108*(A2), 1070, doi:10.1029/2002JA009474.

Intriligator, D. S., and G. L. Siscoe (1994), Stream interfaces and energetic ions closer than expected: Analyses of Pioneer 10 and 11 observations, *Geophys. Res. Lett.*, *21*(12), 1117–1120.

Intriligator, D. S., and G. L. Siscoe (1995), Cross-field diffusion in corotating interaction regions, *J. Geophys. Res.*, *100*(A11), 21,605–21,612.

Intriligator, D. S., G. L. Siscoe, G. Wibberenz, H. Kunow, and J. T. Gosling (1995), Stream interfaces and energetic ions 2. Ulysses test of Pioneer results, *Geophys. Res. Lett.*, *22*(10), 1173–1176.

Intriligator, D. S., J. R. Jokipii, T. S. Horbury, J. M. Intriligator, R. J. Forsyth, H. Kunow, G. Wibberenz, and J. T. Gosling (2001), Processes associated with particle transport in corotating interaction regions and near stream interfaces, *J. Geophys. Res.*, *106*(A6), 10,625–10,634.

Intriligator, D. S., W. Sun, M. Dryer, C. D. Fry, C. Deehr, and J. Intriligator (2005), From the Sun to the outer heliosphere: Modeling and analyses of the interplanetary propagation of the October/November (Halloween) 2003 solar events, *J. Geophys. Res.*, *110*(A9), A09S10, doi:10.1029/2005JA010939.

Intriligator, D., W. Sun, T. Detman, M. Dryer, C. Fry, C. Deehr, and J. Intriligator (2006), Solar variability effects in the outer heliosphere and heliosheath, in *Physics of the Inner Heliosheath*, edited by J. Heerikhuisen, *Amer. Inst. of Phys. Conf. Proc.*, *858*, 64–70.

Jones, G. H., and A. Balogh (2000), Context and heliographic dependence of heliospheric planar magnetic structures, *J. Geophys. Res.*, *105*(A6), 12,713–12,724.

Jones, G. H., and A. Balogh (2001), Planar structuring of magnetic fields at solar minimum and maximum, *Space Sci. Rev.*, *97*, 165–168.

Jones, G. H., A. Balogh, and T. S. Horbury (1999), Observations of heliospheric planar and offset-planar magnetic structures, *Geophys. Res. Lett.*, *26*(1), 13–16.

McDonald, F. (2006), *Edward C. Stone Symposium*, Pasadena, CA, February.

McDonald, F. B., W. R. Webber, E. C. Stone, A. C. Cummings, B. C. Heikikla, and N. Lal (2006), The temporal and spatial variations of galactic and anomalous cosmic rays in the heliosheath, in *Physics of the Inner Heliosheath*, edited by J. Heerikhuisen, *Amer. Inst. of Phys. Conf. Proc.*, *858*, 79–85.

Nakagawa, T., A. Nishida, and T. Saito (1989), Planar magnetic structures in the solar wind, *J. Geophys. Res.*, *94*(A9), 11,761–11,775.

Sonnerup, B. U. O., and L. J. Cahill Jr. (1967), Explorer 12 observations of the magnetopause current layer, *J. Geophys. Res.*, *73*, 1757–1770.

Wibberenz, G., I. G. Richardson, and H. Cane (2002), A simple concept for modeling cosmic ray modulation in the inner heliosphere during solar cycles 20–23, *J. Geophys. Res.*, *107*(A11), 1353, doi:10.1029/2002JA009461.

T. S. Horbury and A. Rees, The Blackett Laboratory, Imperial College London, SW7 2AZ, UK.

D. S. Intriligator, Carmel Research Center, P.O. Box 1732, Santa Monica, CA 90406, USA. (devriei@aol.com)